Effect of high-frequency low-intensity pulsed electric field on protecting SH-SY5Y cells against hydrogen peroxide and β-amyloid-induced cell injury via ERK pathway

Wei-Ting Chen[1,2,¶], Guan-Bo Lin[1,2,¶], Yu-Yi Kuo[1,2,¶], Chih-Hsiung Hsieh[1,2], Chueh-Hsuan Lu[1,2], Yi-Kun Sun[2], and Chih-Yu Chao[1,2,3,*]

[1] Department of Physics, Lab for Medical Physics & Biomedical Engineering, National Taiwan University, Taipei 10617, Taiwan

[2] Biomedical & Molecular Imaging Center, National Taiwan University College of Medicine, Taipei 10051, Taiwan

[3] Graduate Institute of Applied Physics, Biophysics Division, National Taiwan University, Taipei 10617, Taiwan

* Corresponding author

E-mail: cychao@phys.ntu.edu.tw (CYC)

¶ These authors contributed equally to this work.

Abstract

As the most common type of neurodegenerative diseases (NDDs), Alzheimer's disease (AD) is thought to be caused mainly by the excessive aggregation of β-amyloid protein (Aβ). However, a growing number of studies have found that reactive oxygen species (ROS) play a key role in the onset and progression of AD. The present study aimed to probe the neuroprotective effect of high-frequency low-intensity pulsed electric field (H-LIPEF) for SH-SY5Y cells against hydrogen peroxide (H_2O_2) and Aβ-induced cytotoxicity. By looking in a systematic way into the frequency- and amplitude-dependent neuroprotective effect of pulsed electric field (PEF), the study finds that H-LIPEF at 200 Hz produces the optimal protective effect for SH-SY5Y cells. The underlying mechanisms were confirmed to be due to the activation of extracellular signal-regulated kinase (ERK) pathway and the downstream prosurvival and antioxidant proteins. Given that electric field can be modified to focus on specific area for application in a non-contact manner, the study proposes that H-LIPEF holds great potential for neuroprotection and curing of NDDs patients, whose effect can be further augmented with the administering of drugs or natural compounds at the same time.

Introduction

Neurodegenerative diseases (NDDs) feature progressive deterioration of brain function, resulting from the gradual degeneration or death of neurons. Along with increasing human lifespan, deaths caused by NDDs have been on the rise over the past years, impacting the quality of life of patients and their families. The World Health Organization (WHO) predicts that by 2040, NDDs will overtake cancer to be the second leading cause of death, next to cardiovascular diseases.

As the most common kind of neurodegenerative disorder among various NDDs, Alzheimer's disease (AD) displays such typical symptoms as the deposition of cortical plaques, formed by aggregation of β-amyloid protein (Aβ) or hyperphosphorylation of Tau protein, leading to the formation of neurofibrillary tangles ultimately [1]. Scientists have long suspected that these abnormal structures are major culprit in damaging and killing nerve cells, which causes progressive brain degeneration and deterioration of cognitive function among elderly people. In addition, there have been increasing amount of evidences showing that ROS plays a central role in the onset and progression of AD [2]. Therefore, drugs or treatments which could decrease the ROS level and protect neural cells against oxidative damage may be potential strategies to treat AD. Some in vitro or in vivo studies have explored the curative effect of

antioxidant and antiapoptotic drugs in AD treatment [3-5]. However, there has yet to be a cure for AD or other kinds of NDDs. Existing medications can only avoid deterioration of symptoms or postpone their appearance at best. One blockade in AD drug development is the blood-brain barrier (BBB), which is insurmountable for 98% of small molecule drugs and 100% of large molecule drugs [6]. Therefore, effective AD treatment remains a major challenge for modern medicine.

In our previous study, non-invasive low-intensity pulsed electric field (LIPEF) was employed, in conjunction with fucoidan, in preventing oxidative stress-induced mouse motor neuron death [7]. It found that LIPEF suppressed the hydrogen peroxide (H_2O_2)-enhanced expression of ROCK protein and increased the phosphorylation of Akt in H_2O_2-treated NSC-34 cell line. The current study employed non-contact LIPEF stimulation in studying human neural cell line SH-SY5Y, a neurodegenerative damage model with extensive application, and probed the neuroprotective effect of LIPEF against oxidative damage caused by H_2O_2. It also applied AD disease model by Aβ protein administration in neuroprotective study. Interestingly, the study finds that the LIPEF parameters applied in mouse motor neuron are not effective in human neural cell line. The systematic study on frequency- and amplitude-dependent neuroprotective effect of LIPEF was performed, and the result found that high-frequency LIPEF (H-LIPEF) at 200 Hz had the optimal protective effect for

SH-SY5Y cells. Since the alternating current (AC) signal has only one frequency and intensity, it needs time-consuming and painstaking effort for finding the specific AC electric signal to achieve a certain biological effect. Therefore, the approach has only limited applicability, as the specific AC signal is by no means sufficient in targeting complex signal transductions in a biological process or disease treatment. By contrast, the pulsed electric field (PEF) features a composition of multiple sinusoidal subcomponents with diverse frequencies and intensities simultaneously [7]. The study points out that thanks to its multi-frequency components, PEF can facilitate significantly the development of new disease therapeutics in fulfilling different demands.

In the study, we applied the H-LIPEF stimulation to human neural cell line SH-SY5Y, and examined the prosurvival effect of such physical stimulation against oxidative damage caused by H_2O_2 and Aβ-induced cytotoxicity. The results found that exposure of the cells to H-LIPEF at 200 Hz significantly ameliorated the H_2O_2- and Aβ-induced cytotoxicity in SH-SY5Y cells. Examination of the underlying mechanism also showed that 200 Hz H-LIPEF could activate extracellular signal-regulated kinase (ERK) pathway and downstream neuroprotective proteins. These findings imply that H-LIPEF is a promising electrotherapy, shedding light on a novel approach in treatment of AD or other NDDs.

Materials and methods

Experimental setup for exposure of the cells to non-contact H-LIPEF

The LIPEF device described previously [7] was used for exposure of electric field with various strengths and frequencies. The cells were placed between two copper flat and parallel electrodes. Consecutive pulses with pulse duration 2 ms, different electric field intensities and different frequencies were applied across the electrodes. Cells treated with continuous LIPEF were kept in a humidified incubator of 5% CO_2 and 95% air at 37°C. After optimization of the pulse parameters, we used the H-LIPEF stimulation to produce the electric field in a non-contact manner, and examined its neuroprotection effect against the oxidative insult caused by H_2O_2 to SH-SY5Y human neural cells.

Cell culture and treatment

The SH-SY5Y cell was purchased from Bioresource Collection and Research Center (Hsinchu, Taiwan) and maintained in MEM/F-12 mixture containing 10% fetal bovine serum (HyClone; GE Healthcare Life Sciences) and 1% penicillin-streptomycin, supplemented with 1 mM sodium pyruvate and 0.1 mM non-essential amino acids.

Cells were maintained in a humidified incubator composed of 5% CO_2 and 95% air at 37°C. Cells were harvested with 0.05% trypsin–0.5 mM EDTA solution (Gibco; Thermo Fisher Scientific, Inc.) and prepared for in vitro experiments. Cells were pretreated with H-LIPEF for 4 h and then challenged with 500 μM H_2O_2 in the continuous administration of H-LIPEF for another 24 h. For the AD disease model, the cells were pretreated with H-LIPEF for 4 h and then challenged with 25 or 50 μM $A\beta_{25-35}$ protein solution in the continuous administration of H-LIPEF for another 4 days. The Aβ stock solution was prepared by solubilizing the $A\beta_{25-35}$ peptide (Sigma-Aldrich; Merck KGaA) in sterile deionized water to a concentration of 1 mM and then incubated at 37°C for 3 days to allow self-aggregation before treatment. After the treatment, the cell viability was determined. For the ERK inhibitor experiment, 50 μM PD98059 (Cell Signaling Technology, Inc.) was treated 1 h before the H-LIPEF treatment.

Cell viability assay

Viability of SH-SY5Y cells after treatments with or without H-LIPEF was assessed by 3-(4,5-dimethylthiazol-2-yl)-2,5-diphenyltetrazolium bromide (MTT) (Sigma-Aldrich; Merck KGaA) assay. Briefly, the medium was replaced with MTT solution (0.5 mg/mL in SH-SY5Y culture medium) and incubated at 37°C for 4 h.

During this period, the ability of mitochondrial dehydrogenases to reduce the MTT to formazan crystal is an indicator of cellular viability. Following MTT reaction, formazan dissolution was performed by using 10% sodium dodecyl sulfate (SDS) and 0.01 M HCl. The optical density of each well was then determined at 570 nm subtracting the background at 690 nm using an ELISA microplate reader. The cell viability was calculated based on the intensity of formazan, and expressed as percentage of the non-treated control.

ROS level detection

After the treatments, the SH-SY5Y cells were collected and the ROS levels were detected using the fluorescent dye dihydroethidium (DHE) (Sigma-Aldrich; Merck KGaA). Cells were incubated with 5 μM DHE dye for 20 min at 37°C in the dark and then the fluorescence intensity was measured by flow cytometry in the PE channel. The ROS levels were expressed as mean fluorescence intensity for comparison.

Mitochondrial membrane potential (MMP) measurement

The detection of MMP was carried out by flow cytometry using 3,3'-dihexyloxacarbocyanine iodide [$DiOC_6(3)$] (Enzo Life Sciences International Inc.). $DiOC_6(3)$ is a lipophilic cationic fluorescent dye which is selective for the

mitochondria of live cells. It allows estimation of the percentage of cells with depleted MMP which reflects the initiation of proapoptotic signal. Cells treated with H_2O_2 and H-LIPEF alone or in combination for 24 h were harvested and suspended in PBS with 20 nM $DiOC_6(3)$. After incubation at 37°C for 15 min in the dark, the fluorescence intensity was immediately measured by flow cytometry.

Western blot analysis

After the treatments, cells were washed with phosphate buffered saline (PBS) and then harvested and lysed in RIPA lysis buffer (EMD Millipore) containing fresh protease and phosphatase inhibitor cocktail (EMD Millipore). The lysates were then centrifuged, and the supernatant was collected and used for the determination of protein concentration. Equal amounts of protein extracts were loaded in the 10% SDS-PAGE wells and transferred to polyvinylidene fluoride membranes. After drying for 1 h at room temperature (RT), the membranes were probed with ROCK (Abcam, plc.), p-ERK, Nrf2, p-CREB, Bcl-2, Bax (Cell Signaling Technology, Inc.), and GAPDH (GeneTex, Inc.) antibodies overnight at 4˚C. Subsequently, the washed membranes were incubated with horseradish peroxidase-coupled secondary antibodies (Jackson ImmunoResearch Laboratories, Inc.) for 1 h at RT. All the antibodies were diluted at the optimal concentration according to the manufacturer's instructions.

Finally, protein bands were visualized with an enhanced chemiluminescence substrate (Advansta, Inc.) and detected with the Amersham Imager 600 imaging system (GE Healthcare Life Sciences). The images were analyzed with Image Lab software (Bio-Rad Laboratories, Inc.). For normalization of proteins, GAPDH was used as an internal control.

Statistical analysis

Each data point represents the average from larger or equal to three independent experiments and is expressed as the mean ± standard deviation. Statistical analyses were performed using OriginPro 2015 software (OriginLab). Differences of statistical significance were determined by a one-way analysis of variance (ANOVA), followed by Tukey's post-hoc test. P-value < 0.05 was considered to indicate a statistically significant difference.

Results

In vitro-applied H-LIPEF

The H-LIPEF was applied in a non-contact manner with the apparatus consisting of two thin parallel conductive electrodes mounted on the insulating acrylic frame (Fig

1A). The culture dishes were placed between the parallel electrodes so the cells were not in contact with the electrodes directly. Therefore, the H-LIPEF stimulation device can provide the electric field in a non-invasive manner, avoiding the harmful effects caused by conduction current and Joule effect via contact electrodes. The pulsed electric signal was from a function generator and amplified by a voltage amplifier. In the study, the applied electric signal was characterized by a pulse train waveform (Fig 1B) with various field intensities (1-60 V/cm) and frequencies (2-499 Hz) for optimization of the treatment.

Fig 1. The experimental setup of H-LIPEF. (A) Image of the H-LIPEF stimulation device. The culture dishes were placed in the stimulation device constructed of two parallel electrodes. The blue arrows shown here indicate the schematic representation of non-invasive H-LIPEF exposure on cells. (B) Schematic representation of the pulse train waveform applied on the electrodes.

Effect of H-LIPEF exposure on H_2O_2- and Aβ-induced cytotoxicity in SH-SY5Y cells

The oxidative stress plays a critical role in the etiology and exacerbates the NDDs progression. We applied H_2O_2 to SH-SY5Y cells as an oxidative stress and looked

into the neuroprotective effect of H-LIPEF technique. As shown in Fig 2A, administration of H_2O_2 on SH-SY5Y cells for 24 h decreased the cell viability in a dose-dependent manner. Treatment of SH-SY5Y cells with 500 μM H_2O_2 for 24 h reduced the cell viability to 52% compared to the control cells, which was used in the subsequent experiments. To examine whether H-LIPEF could produce protection and increase the cell viability against the oxidative insult, cells were pretreated with H-LIPEF for 4 h and then exposed to H_2O_2 in the continuous administration of H-LIPEF for another 24 h. In our previous study, the low frequency LIPEF with parameters of 2 Hz, 60V/cm, and 2 ms pulse duration was used in the mouse motor neurons NSC-34 [7], but the result showed that this parameter combination is ineffective in the SH-SY5Y cells. In this study, we used H-LIPEF in our experiments, and found that the H-LIPEF stimulation using the parameters of 200 Hz, 10 V/cm, and 2 ms pulse duration produced significant protection against the oxidative insult caused by H_2O_2 to SH-SY5Y human neural cell line (Fig 2B). To examine whether the frequency and intensity are both critical parameters in the neuroprotective effect, the systematic study on frequency- and amplitude-dependent effects was performed. The intensity of H-LIPEF was firstly fixed at 10 V/cm and the frequency was varied from 2 Hz to 499 Hz. The upper limit was set to 499 Hz since for 2 ms pulse duration, two pulses will overlap for frequency greater or equal to 500 Hz. The results showed that

for frequency less than or equal to 100 Hz, their survival rates were not significantly different from the H_2O_2-treated group. At high frequency region, the H-LIPEF conferred protective effect to the H_2O_2-treated SH-SY5Y cells, and the maximum protective effect was at near 200 Hz (Fig 2C). For the intensity-dependent effect, the frequency was fixed at 200 Hz, and the intensity varied from 1~60 V/cm was examined. As shown in Fig 2D, it was obvious that there was a maximum at 10 V/cm, indicating that the best protective effect was at 10 V/cm. Therefore, we conclude that both the frequency and intensity are critical parameters in the neuroprotective effect, and the optimum protective parameters (200 Hz, 10 V/cm, and 2 ms pulse duration) were used in the following experiments. For AD disease model, it was found that Aβ treatment reduced the viability of SH-SY5Y cells due to the cytotoxicity of the aggregated Aβ (Fig 3A). As shown in Fig 3B and 3C, the H-LIPEF treatment greatly improved the viability and restored the cell morphology of Aβ-treated SH-SY5Y cells, indicating the curative effect of H-LIPEF in AD disease model in vitro.

Fig 2. Effect of H-LIPEF on H_2O_2-induced cytotoxicity in SH-SY5Y cells. (A) Dose-dependent curve of SH-SY5Y cells treated with different concentrations of H_2O_2 and the cell viability was measured by MTT assay at 24 h after the H_2O_2 treatment. (B) SH-SY5Y cells were pretreated using 200 Hz H-LIPEF with field

intensity of 10 V/cm and challenged with or without 500 μM H_2O_2. The cell viability was also measured by MTT assay at 24 h after the H_2O_2 treatment. (C) SH-SY5Y cells were pretreated with 10 V/cm PEF at different pulse frequencies and challenged with 500 μM H_2O_2 for 24 h and then the cell viability was measured by MTT assay. (D) SH-SY5Y cells were pretreated using 200 Hz PEF with different field intensities and challenged with 500 μM H_2O_2 for 24 h and then the cell viability was measured by MTT assay. Data represent the mean ± standard deviation (n=3). $^{***}P < 0.001$.

Fig 3. Effect of H-LIPEF on Aβ-induced cytotoxicity in SH-SY5Y cells. (A) The cell viability of SH-SY5Y cells treated with 25 or 50 μM Aβ for 4 days. (B) The SH-SY5Y cells were pretreated with H-LIPEF for 4 h and then exposed to 50 μM Aβ in the continuous administration of H-LIPEF for another 4 days, and the cell viability was measured by MTT assay. (C) Representative light microscopy images of SH-SY5Y cells after Aβ and/or H-LIPEF treatment. The integrity of the cells was destructed by Aβ, and the H-LIPEF treatment caused the protective effect and retained the cell morphology. Scale bar = 100 μm. Data represent the mean ± standard deviation (n=3). $^{***}P < 0.001$.

H-LIPEF attenuates H_2O_2-induced ROS generation

Since the onset of AD is associated with ROS accumulation, we further examined the effect of H-LIPEF on the ROS level regulation by flow cytometry (Fig 4A). Quantification results (Fig 4B) showed that the ROS level was increased to 175% of the control level after exposure to 500 μM H_2O_2 for 24 h. Compared to the group of H_2O_2 alone, the H-LIPEF treatment greatly ameliorated the H_2O_2-induced ROS level elevation, indicating that H-LIPEF could have the ability to decrease the ROS level.

Fig 4. Effect of H-LIPEF on H_2O_2-induced ROS generation in SH-SY5Y cells. (A) ROS level was measured by flow cytometry with DHE fluorescent dye. (B) Quantification of the ROS levels after H-LIPEF, H_2O_2, or H-LIPEF+H_2O_2 treatment. Data represent the mean ± standard deviation (n=3). $^{***}P < 0.001$.

H-LIPEF attenuates MMP loss in H_2O_2-treated cells

Many research evidences have suggested that mitochondria play important roles in NDDs through the accumulation of net cytosolic ROS production [8]. In healthy cells, the levels of MMP are kept relatively stable, and the depletion of MMP suggests the loss of mitochondrial membrane integrity. Apoptotic signals are usually initiated by such mitochondrial dysfunctions. To examine whether the neuroprotective effect of H-LIPEF is associated with mitochondrial functions, the MMP is further analyzed by

the flow cytometry with $DiOC_6(3)$ fluorescent dye. As shown in Fig 5A, it was found that H_2O_2 caused mitochondrial dysfunction, decreasing the MMP and therefore decreased the intensity of the $DiOC_6(3)$ fluorescent signal while H-LIPEF alone did not change the MMP. From the quantification results (Fig 5B), we found that the cells with decreased MMP drastically increased after the H_2O_2 treatment, and H-LIPEF pretreatment noticeably suppressed the H_2O_2-induced dissipation of MMP, so the cells with decreased MMP reduced significantly. The results indicate that H-LIPEF could prevent the mitochondria from damaging by the oxidative stress and thus caused the blockage of the apoptotic signaling transduction.

Fig 5. Effect of H-LIPEF on H_2O_2-induced MMP reduction in SH-SY5Y cells. (A) MMP was analyzed by flow cytometry with $DiOC_6(3)$ fluorescent dye. (B) Quantification of the cells with decreased MMP after H-LIPEF, H_2O_2, or H-LIPEF+H_2O_2 treatment. Data represent the mean ± standard deviation (n=3). $^{**}P < 0.01$.

Effect of H-LIPEF treatment on ROCK protein expression in SH-SY5Y cells

In our previous study, the neuroprotective effect of LIPEF was found to be associated

with the inhibition of the H_2O_2-induced activation of ROCK pathway in the motor neuron cell line NSC-34 [7]. In this work, we examined the ROCK protein expressions in order to investigate whether the protective effect of high frequency LIPEF on human neuroblastoma SH-SY5Y cells was related to the ROCK pathway. As shown in Fig 6, the expression of ROCK protein is slightly higher after H_2O_2 treatment but almost unaffected after the treatment of both H-LIPEF and H_2O_2. This phenomenon points out that although the H-LIPEF treatment can protect SH-SY5Y cells, the main mechanism is not associated with the ROCK pathway. Therefore, other prosurvival protein pathways should be considered in the following experiments.

Fig 6. Effect of H-LIPEF on expressions of ROCK protein in SH-SY5Y cells. (A) Western blot analysis of ROCK protein expressions. (B) Quantification of ROCK expression level after H-LIPEF, H_2O_2, or H-LIPEF+H_2O_2 treatment. The expression levels were normalized to GAPDH and each relative expression level was compared with control. Data represent the mean ± standard deviation (n=3).

Effect of H-LIPEF exposure on ERK-Nrf2/CREB signalling pathways in H_2O_2-treated SH-SY5Y cells

We then studied the signalling pathways that could participate in the neuroprotective

mechanism of H-LIPEF stimulation. ERK is one of the major cascades of mitogen-activated protein kinases (MAPK) family and has been known to be widely associated with cell survival [9]. Upon phosphorylation, the active ERK proteins enter into the nucleus where they can phosphorylate certain transcription factors, thus regulating the expression of specific genes that contribute to cell survival [10]. Therefore, in our study, we examined the phosphorylation of ERK and the downstream transcription factors including cAMP response element binding protein (CREB) and nuclear factor erythroid 2-related factor 2 (Nrf2) by western blot analysis.

As shown in Fig 7A, in comparison to the untreated control cells, the level of phosphorylated ERK (p-ERK) was increased in the cells exposed to H-LIPEF for 24 h. In contrast, the level of p-ERK in the cells was decreased when exposed to 500 μM H_2O_2 for 24 h without the treatment of H-LIPEF. In addition, the result showed that the H-LIPEF treatment induced a significant recovery of the p-ERK level in the cells exposed to 500 μM H_2O_2. This result indicates that the neuroprotection provided by H-LIPEF could be related to the recovery of the H_2O_2-induced decline of p-ERK. In the following, we further examined the expression levels of Nrf2 and p-CREB proteins using western blot analysis. Nrf2 is a key transcription factor that regulates the expression of antioxidant proteins participating in the protection of oxidative

damage triggered by injury and inflammation. As shown in Fig 7B, the level of Nrf2 was also increased in H-LIPEF treated SH-SY5Y cells compared to the untreated cells. In contrast, the level of Nrf2 in the cells exposed to 500 μM H_2O_2 for 24 h but without the treatment of H-LIPEF was decreased. Meanwhile, the H-LIPEF treatment was found to recover the expression of Nrf2 in the cells exposed to 500 μM H_2O_2 obviously. This result showed that the neuroprotective effect was due in part to the H-LIPEF induced Nrf2 expression and the antioxidant effect. Next, CREB is also an important transcription factor triggering the expression of prosurvival proteins. As shown in Fig 7C, in comparison to the untreated control cells, the level of p-CREB was dramatically increased when cells were under the H-LIPEF treatment alone. On the other hand, the level of p-CREB in cells was decreased when exposed to 500 μM H_2O_2 for 24 h without the treatment of H-LIPEF. Moreover, the result found that the H-LIPEF treatment obviously recovered the expression of p-CREB in the cells exposed to 500 μM H_2O_2. Furthermore, it is widely known that CREB phosphorylation regulates Bcl-2 family proteins including anti-apoptotic Bcl-2 and pro-apoptotic Bax proteins, and the ratio of Bcl-2/Bax determines whether neurons undergo survival or death after an apoptotic stimulus. Therefore, the expressions of Bcl-2 and Bax protein levels were also examined in the study. As shown in Fig 7D, for SH-SY5Y cells under the H-LIPEF treatment alone, the expression levels of Bcl-2

and Bax were increased and decreased respectively, leading to a higher elevation of the Bcl-2/Bax ratio compared to the untreated control cells. Meanwhile, in comparison to the untreated control cells, the level of Bcl-2/Bax ratio of SH-SY5Y cells was found to decrease when exposed to 500 μM H_2O_2, indicating that the cells had undergone apoptosis. Moreover, it was observed that the H-LIPEF treatment notably restored the expression of Bcl-2/Bax ratio in the cells exposed to 500 μM H_2O_2. To sum up, the results showed that the H-LIPEF treatment induced the anti-apoptotic effect by regulating the Bcl-2 family proteins via modulating the ERK/CREB pathways and thus promoted the cell survival against oxidative stress.

Fig 7. Effect of H-LIPEF on ERK/Nrf2 and ERK/CREB signalling pathways and related protein expressions. Western blot analysis of p-ERK (A), Nrf2 (B), p-CREB (C), Bcl-2 and Bax (D) protein expressions. The expression levels were normalized to GAPDH and each relative expression level was compared with control. Data represent the mean ± standard deviation (n=3). $^{***}P < 0.001$ and $^{**}P < 0.01$.

Effect of PD98059 on the H-LIPEF activated ERK pathway and protective effect

To confirm the neuroprotective effect of H-LIPEF is related to the ERK pathway, we inhibited the MAPK kinases MEK1 and MEK2, the upstream kinases of ERK, by the inhibitor PD98059 [11] in the study. In Fig 8A, we found that H-LIPEF could significantly increase the cell viability of SH-SY5Y cells to about 80% of the control level under H_2O_2 stress. In the presence of MEK inhibitor, the p-ERK level was indeed reversed and the neuroprotective effect of H-LIPEF treatment against H_2O_2-induced cell apoptosis was abrogated (Fig 8A and 8B). The results indicate that the ERK pathway was involved to mediate the neuroprotective effect of H-LIPEF treatment against H_2O_2 toxicity. On the whole, the data point out that H-LIPEF treatment may produce neuroprotective effect via activation of the ERK signalling pathway in the H_2O_2-treated SH-SY5Y human neural cells.

Fig 8. Effect of PD98059 on the neuroprotective effect of H-LIPEF and p-ERK protein expression induced by H-LIPEF stimulation. (A) H-LIPEF increased the cell viability of SH-SY5Y cells under H_2O_2 oxidative stress. The neuroprotective effect of H-LIPEF treatment was abrogated by addition of the MEK inhibitor PD98059. (B) The western blot analysis showed that the inhibitor PD98059 reversed the activated level of p-ERK induced by H-LIPEF treatment. The expression levels were normalized to GAPDH. We used the abbreviation “PD” to represent the MEK

inhibitor PD98059 in the figure. Data represent the mean ± standard deviation (n=3). $^{**}P < 0.01$.

Discussion

The focus of this study was to probe the neuroprotective effect of H-LIPEF on SH-SY5Y cells. The results demonstrated that application of high-frequency (~200 Hz) and low-intensity (~10 V/cm) pulsed electric field produced the most significant protection for SH-SY5Y human neural cells against H_2O_2- and Aβ-induced apoptosis. The western blot results exhibited that H-LIPEF triggered the ERK signalling pathway and mediated the activation of CREB and Nrf2 transcription factors.

As the most common form of age-related NDDs, AD features excessive aggregation of Aβ and intracellular microtubule-associated protein tau, known as neurofibrillary tangles. With many questions remaining unanswered, some researchers believe that the amyloid cascade hypothesis offers the best explanation for the cause of AD [12], maintaining that Aβ is the causative factor of Alzheimer's pathology and that the neurofibrillary tangles, cell loss, vascular damage, and dementia all result directly from such deposition. Although the mechanism of Aβ-induced cytotoxicity has yet to be elucidated completely, several studies have proven that the oxidative stress plays a vital role in Aβ-induced apoptosis [13-15]. Therefore, researchers have

been striving to find various antioxidants that can protect against oxidative stress and alleviate the symptoms of NDDs [16-18]. However, the therapeutic effect of most antioxidant compounds is limited, due to their incapability to cross the BBB. Among different ROS species, H_2O_2 is one of the molecules most related to the progression of AD. In the study, H_2O_2 was applied as the oxidative stress which caused cell death at certain dosage. The results found that H_2O_2 treatment increased the ROS level and H-LIPEF treatment significantly ameliorated the H_2O_2-induced ROS level elevation, underscoring the antioxidant ability of H-LIPEF. The study employed MTT and MMP assays to assess the cell viability and mitochondria integrity, finding in both results that H-LIPEF provided the neuroprotective effect and increased the viability and MMP in the H_2O_2-treated neural cells. Furthermore, Aβ was used to investigate the neuroprotective effect of H-LIPEF in the AD disease model. The MTT and light microscopy results also showed that H-LIPEF greatly improved the viability and retained the cell integrity in the Aβ-treated cells. Since the electric field can penetrate the human body without the restriction of BBB, H-LIPEF promises a potent alternative therapeutic medicine in NDDs treatment.

The electric stimulation has a long history of medical applications, including wound healing [19], muscle relaxation [20], and increase of blood circulation [21], often involving passage of electric current through the injury parts via direct contact

between the body and implanted electrodes. However, the invasive or contact manner significantly dampens the feasibility of the treatment or even causes harms to cells or body, such as electrolysis, burns and muscle spasms [22]. Therefore, it is desirable for electrotherapy to be carried out in a non-invasive or non-contact manner. Our previous study demonstrated a non-contact electric stimulation device [23], which operates as a parallel capacitor generating electric field between two parallel electrodes (Fig 1A). Therefore, the electric field with such capacitive coupling mode can pass through biological samples to achieve specific biological effect without current actually flowing through cells or media via contact with electrodes. It is noteworthy that the strength of electric field passing through culture dishes or media is the same as the voltage for electrodes. Besides, the electric field waveform employed was a PEF, which is characterized by its multi-frequency component nature. Pulse train signal is composed of multiple sinusoidal subcomponents with different frequencies and intensities [7]. When PEF enters a biological sample, it encounters different proteins, cells and tissues with different dielectric constants and is therefore dispersed to multiple frequencies electrically. Multi-frequency sinusoidal waves may interact with molecules, proteins, or organelles simultaneously to induce specific bioeffect in the PEF exposure. In our previous studies, the non-contact LIPEF exhibited promising potential in activating anticancer agent in pancreatic cancer

treatment [24] and also in the neuroprotection of mouse motor neurons [7]. In the current study, LIPEF with different parameters was applied to the human neural cells for examination of its neuroprotective effect. Unexpectedly, the LIPEF parameter applied in mouse motor neurons NSC-34 turned out to be ineffective for human SH-SY5Y cells. In fact, scientists have found that mouse-based model is not applicable to humans [25], which provides the reason why some drugs or treatments that successfully treat mice do not work for people. Therefore, it is critical to find treatments for animal models or cell types closely related to humans. The study found that for human SH-SY5Y cells, the neuroprotective effect of LIPEF was more pronounced in the high-frequency region, especially near 200 Hz, quite different from the parameter at 2 Hz for NSC-34 mouse cell line. For higher-frequency LIPEF, it consists more high-frequency components in its composition. Therefore, the neuroprotective effect of H-LIPEF for human SH-SY5Y neural cells may be attributable to the employment of high-frequency components participating in the treatment. The results also showed that the therapeutic window of the H-LIPEF intensity for SH-SY5Y cells was near 10 V/cm, which was smaller than the most effective parameter (60 V/cm) for NSC-34 cells. Therefore, it is evident that the pulse frequency and the field intensity are critical parameters for therapeutic applications. The parameters (frequency, intensity, and pulse duration) of LIPEF need to be

fine-tuned and optimized for different types of cells or diseases. Furthermore, the study proposes combination of multiple pulses with different parameters to treat the targeted region simultaneously.

As for the neuroprotective mechanism, it was found previously that the LIPEF treatment obviously suppressed the H_2O_2-enhanced expression of ROCK protein in NSC-34 cells. However, for SH-SY5Y cells, the H-LIPEF simulation did not have significant impact on ROCK protein expression. It is thus known that the neuroprotective mechanism is not through the ROCK pathway. In the western blot results, the study proved that such neuroprotective effect induced by H-LIPEF was through activation of ERK pathway. The ERK pathway plays an important role in regulating of proliferation and differentiation as well as survival of various cell types [26]. It transmits external cues, including growth factors into signalling cascade via the phosphorylation of ERK. Several studies have suggested that the stimulation of ERK pathway may be a potential way for neuroprotection [9, 10]. Here, the study showed that the physical stimulation by H-LIPEF alone significantly enhanced the expression level of p-ERK, indicating H-LIPEF could activate the ERK signalling pathway. Since the ERK pathway is initiated by the binding of epidermal growth factor (EGF) to the epidermal growth factor receptor (EGFR), we speculate that H-LIPEF could have an interaction with EGFR and cause the conformation change of

EGFR, thus triggering the ERK pathway. Previous study had shown that magnetic field could alter the conformation of TRPV1 ion channel, making it more favorable for capsaicin binding [27]. The results implicate that the PEF or magnetic field with different parameters could activate different signalling pathways. In the study, H-LIPEF with 200 Hz frequency and 10 V/cm field intensity was found to significantly trigger the ERK pathway and produce the neuroprotective effect. Consequently, the phosphorylation of ERK protein could result in the activation of its kinase activity and lead to phosphorylation of many downstream targets including certain transcription factors containing CREB and Nrf2 required for neuroprotection.

CREB is an important transcription factor activated by phosphorylation from ERK or other kinases. It triggers expression of neurotrophins and antiapoptotic proteins such as brain-derived neurotrophic factor (BDNF) and B-cell lymphoma 2 (Bcl-2) [28]. Besides, CREB downregulation is related to the pathology of AD [29], and thus increasing the CREB expression has been considered as a potential therapeutic strategy for AD. In the study, it was observed that H-LIPEF could increase the level of p-CREB dramatically. Moreover, the result found that the H-LIPEF treatment notably recovered the expression of p-CREB in the cells exposed to 500 μM H_2O_2. On one hand, it is known that CREB phosphorylation regulates Bcl-2 family proteins including anti-apoptotic Bcl-2 and pro-apoptotic Bax proteins. The

antiapoptotic protein, Bcl-2, has been proposed to be a pivotal component for neuroprotection [30]. It suppresses apoptosis by heterodimerizing with Bax protein and neutralizes the effects of Bax. When Bcl-2 is present in excess, cells are protected against apoptosis. It should be also pointed out that when Bax is excessive and the homodimers of Bax dominate, cells are susceptible to programed cell death. Therefore, it is the ratio of Bcl-2 to Bax which determines the fate of a cell [31]. In the results, we found that the H-LIPEF treatment obviously restored the expression of Bcl-2/Bax ratio in the cells exposed to 500 μM H_2O_2, indicating the prosurvival effect of H-LIPEF in SH-SY5Y cells.

Another possible mechanism for neuroprotection of the H-LIPEF stimulation may be associated with the Nrf2 protein. Nrf2 is also an important transcription factor activated by ERK pathway. It regulates the expression of various antioxidant proteins and maintains their redox states in mammalian cells [32]. The results showed that the H-LIPEF treatment obviously recovered the expression of Nrf2 in the cells exposed to 500 μM H_2O_2, indicating that the neuroprotective effect was due in part to the H-LIPEF induced Nrf2 expression and the antioxidant effect.

The study confirmed the neuroprotective effect of H-LIPEF on SH-SY5Y cells. Given that electric field can be modified to focus on a targeted region, it affirms applicability of H-LIPEF treatment for different human organs. Moreover, it found

that H-LIPEF technique can significantly reduce treatment risk and time, thanks to its non-contact and multi-frequency nature. In addition, the study also demonstrated the ability of H-LIPEF in rescuing the Aβ-induced cytotoxicity. Since the accumulation of misfolded proteins in brain is also a typical symptom of some NDDs, the study could shed light on future exploration for optimal LIPEF conditions in the treatment of other NDDs.

In summary, the study demonstrates for the first time that the physical stimulation by H-LIPEF can protect SH-SY5Y human neural cells from H_2O_2- and Aβ-induced cytotoxicity. The underlying molecular mechanism for the neuroprotective effect is partially attributed to the activation of ERK pathway and the function of some downstream proteins, such as CREB, Nrf2, and Bcl-2. Further studies are necessary to ascertain the optimal LIPEF conditions for other NDDs and the involvement of other proteins in the neuroprotective effect. Finally, it proposes coupling H-LIPEF with NDD drugs or natural compounds to attain better curative effect for NDD patients.

Funding

This work was supported by grants from Ministry of Science and Technology (MOST 108-2112-M-002-016 and 105-2112-M-002-006-MY3 to CYC) and Ministry

of Education (MOE 106R880708 to CYC) of the Republic of China. The funders had no role in study design, data collection and analysis, decision to publish, or preparation of the manuscript.

Competing Interests

The authors have declared that no competing interests exist.

Acknowledgments

The authors would like to acknowledge the service provided by the Research Core Facilities 3 Laboratory of the Department of Medical Research at National Taiwan University hospital for use of flow cytometry system.

Author Contributions

Conceptualization: Chih-Yu Chao.

Data Curation: Wei-Ting Chen, Guan-Bo Lin, Yu-Yi Kuo, Chih-Yu Chao.

Formal analysis: Wei-Ting Chen, Guan-Bo Lin, Yu-Yi Kuo, Chih-Hsiung Hsieh, Chueh-Hsuan Lu, Yi-Kun Sun, Chih-Yu Chao.

Funding acquisition: Chih-Yu Chao.

Investigation: Wei-Ting Chen, Guan-Bo Lin, Yu-Yi Kuo, Chih-Yu Chao.

Project Administration: Chih-Yu Chao.

Supervision: Chih-Yu Chao.

Validation: Wei-Ting Chen, Guan-Bo Lin, Yu-Yi Kuo.

Writing – original draft: Wei-Ting Chen, Guan-Bo Lin, Chih-Yu Chao.

Writing – review & editing: Chih-Yu Chao.

References:

1. Ross CA, Poirier MA. Protein aggregation and neurodegenerative disease. Nat Med. 2004; 10:S10-S17.
2. Kim GH, Kim JE, Rhie SJ, Yoon S. The role of oxidative stress in neurodegenerative diseases. Exp Neurobiol. 2015; 24:325-340.
3. Hemming ML, Selkoe DJ. Amyloid beta-protein is degraded by cellular angiotensin-converting enzyme (ACE) and elevated by an ACE inhibitor. J Biol Chem. 2005; 280:37644-37650.
4. Bachurin SO, Bovina EV, Ustyugov AA. Drugs in clinical trials for Alzheimer's disease: the major trends. Med Res Rev. 2017; 37:1186-1225.
5. Alghazwi M, Smid S, Musgrave I, Zhang W. In vitro studies of the neuroprotective activities of astaxanthin and fucoxanthin against amyloid beta (Aβ1-42) toxicity and aggregation. Neurochem Int. 2019; 124:215-224.
6. Yang Y, Zhang X, Ye D, Laforest R, Williamson J, Liu Y, et al. Cavitation dose painting for focused ultrasound-induced blood-brain barrier disruption. Sci Rep. 2019; 9:2840.
7. Hsieh CH, Lu CH, Kuo YY, Lin GB, Chao CY. The protective effect of non-invasive low intensity pulsed electric field and fucoidan in preventing oxidative stress-induced motor neuron death via ROCK/Akt pathway. PLoS One. 2019; 14:e0214100.
8. Manczak M, Anekonda TS, Henson E, Park BS, Quinn J, Reddy PH. Mitochondria are a direct site of Aβ accumulation in Alzheimer's disease neurons: implications for free radical generation and oxidative damage in disease progression. Hum Mol Genet. 2006; 15:1437-1449.

609 9. Mohamed SK, Ahmed AAE, Elmorsy EM, Nofal S. ERK activation by zeranol has
610 neuroprotective effect in cerebral ischemia reperfusion. Life Sci. 2019; 227:137-144.
611 10. Almeida RD, Manadas BJ, Melo CV, Gomes JR, Mendes CS, Grãos MM, et al.
612 Neuroprotection by BDNF against glutamate-induced apoptotic cell death is
613 mediated by ERK and PI3-kinase pathways. Cell Death Differ. 2005; 12:1329-1343.
614 11. Caunt CJ, Sale MJ, Smith PD, Cook SJ. MEK1 and MEK2 inhibitors and cancer
615 therapy: the long and winding road. Nat Rev Cancer. 2015; 15:577-592.
616 12. Karran E, Mercken M, Strooper BD. The amyloid cascade hypothesis for
617 Alzheimer's disease: an appraisal for the development of therapeutics. Nat Rev Drug
618 Discov. 2011; 10:698-712.
619 13. Cheignon C, Tomas M, Bonnefont-Rousselot D, Faller P, Hureau C, Collin F.
620 Oxidative stress and the amyloid beta peptide in Alzheimer's disease. Redox Biol.
621 2018; 14:450-464.
622 14. Butterfield DA, Swomley AM, Sultana R. Amyloid β-peptide (1–42)-induced
623 oxidative stress in Alzheimer disease: importance in disease pathogenesis and
624 progression. Antioxid Redox Signal. 2013; 19:823-835.
625 15. Arimon M, Takeda S, Post KL, Svirsky S, Hyman BT, Berezovska O. Oxidative stress
626 and lipid peroxidation are upstream of amyloid pathology. Neurobiol Dis. 2015;
627 84:109-119.
628 16. Muthaiyah B, Essa MM, Chauhan V, Chauhan A. Protective effects of walnut
629 extract against amyloid beta peptide-induced cell death and oxidative stress in PC12
630 cells. Neurochem Res. 2011; 36:2096-2103.
631 17. Wang C, Li J, Liu Q, Yang R, Zhang JH, Cao Y-P, et al. Hydrogen-rich saline reduces
632 oxidative stress and inflammation by inhibit of JNK and NF-κB activation in a rat
633 model of amyloid-beta-induced Alzheimer's disease. Neurosci Lett. 2011;
634 491:127-132.
635 18. Chan K-H, Lam KS-L, Cheng O-Y, Kwan JS-C, Ho PW-L, Cheng KK-Y, et al.
636 Adiponectin is protective against oxidative stress induced cytotoxicity in
637 amyloid-beta neurotoxicity. PloS One. 2012; 7:e52354-e52354.
638 19. Gentzkow GD, Miller KH. Electrical stimulation for dermal wound healing. Clin
639 Podiatr Med Surg. 1991; 8:827-841.
640 20. Windsor RE, Lester JP, Herring SA. Electrical stimulation in clinical practice.
641 Physician Sportsmed. 1993; 21:85-93.
642 21. Park RJ, Son H, Kim K, Kim S, Oh T. The effect of microcurrent electrical
643 stimulation on the foot blood circulation and pain of diabetic neuropathy. J Phys Ther
644 Sci. 2011; 23:515-518.
645 22. Antov Y, Barbul A, Mantsur H, Korenstein R. Electroendocytosis: exposure of
646 cells to pulsed low electric fields enhances adsorption and uptake of macromolecules.

647 Biophys J. 2005; 88:2206-2223.
648 23. Hsieh CH, Lu CH, Chen WT, Ma BL, Chao CY. Application of non-invasive low
649 strength pulsed electric field to EGCG treatment synergistically enhanced the
650 inhibition effect on PANC-1 cells. PLoS One. 2017; 12:e0188885.
651 24. Lu CH, Lin SH, Hsieh CH, Chen WT, Chao CY. Enhanced anticancer effects of
652 low-dose curcumin with non-invasive pulsed electric field on PANC-1 cells.
653 OncoTargets Ther. 2018; 11:4723-4732.
654 25. Uhl EW, Warner NJ. Mouse models as predictors of human responses:
655 evolutionary medicine. Curr Pathobiol Rep. 2015; 3:219-223.
656 26. Sun Y, Liu WZ, Liu T, Feng X, Yang N, Zhou HF. Signaling pathway of MAPK/ERK in
657 cell proliferation, differentiation, migration, senescence and apoptosis. J Recept
658 Signal Transduct. 2015; 35:600-604.
659 27. Chen WT, Lin GB, Lin SH, Lu CH, Hsieh CH, Ma BL, et al. Static magnetic field
660 enhances the anticancer efficacy of capsaicin on HepG2 cells via capsaicin receptor
661 TRPV1. PLoS One. 2018; 13:e0191078.
662 28. Finkbeiner S. CREB couples neurotrophin signals to survival messages. Neuron.
663 2000; 25:11-14.
664 29. Rosa E, Fahnestock M. CREB expression mediates amyloid β-induced basal BDNF
665 downregulation. Neurobiol Aging. 2015; 36:2406-2413.
666 30. Howard S, Bottino C, Brooke S, Cheng E, Giffard RG, Sapolsky R. Neuroprotective
667 effects of bcl-2 overexpression in hippocampal cultures: interactions with pathways
668 of oxidative damage. J Neurochem. 2002; 83:914-923.
669 31. Pepper C, Hoy T, Bentley DP. Bcl-2/Bax ratios in chronic lymphocytic leukaemia
670 and their correlation with in vitro apoptosis and clinical resistance. Br J Cancer. 1997;
671 76:935-938.
672 32. Kubben N, Zhang W, Wang L, Voss TC, Yang J, Qu J, et al. Repression of the
673 antioxidant NRF2 pathway in premature aging. Cell. 2016; 165:1361-1374.

Figure 1

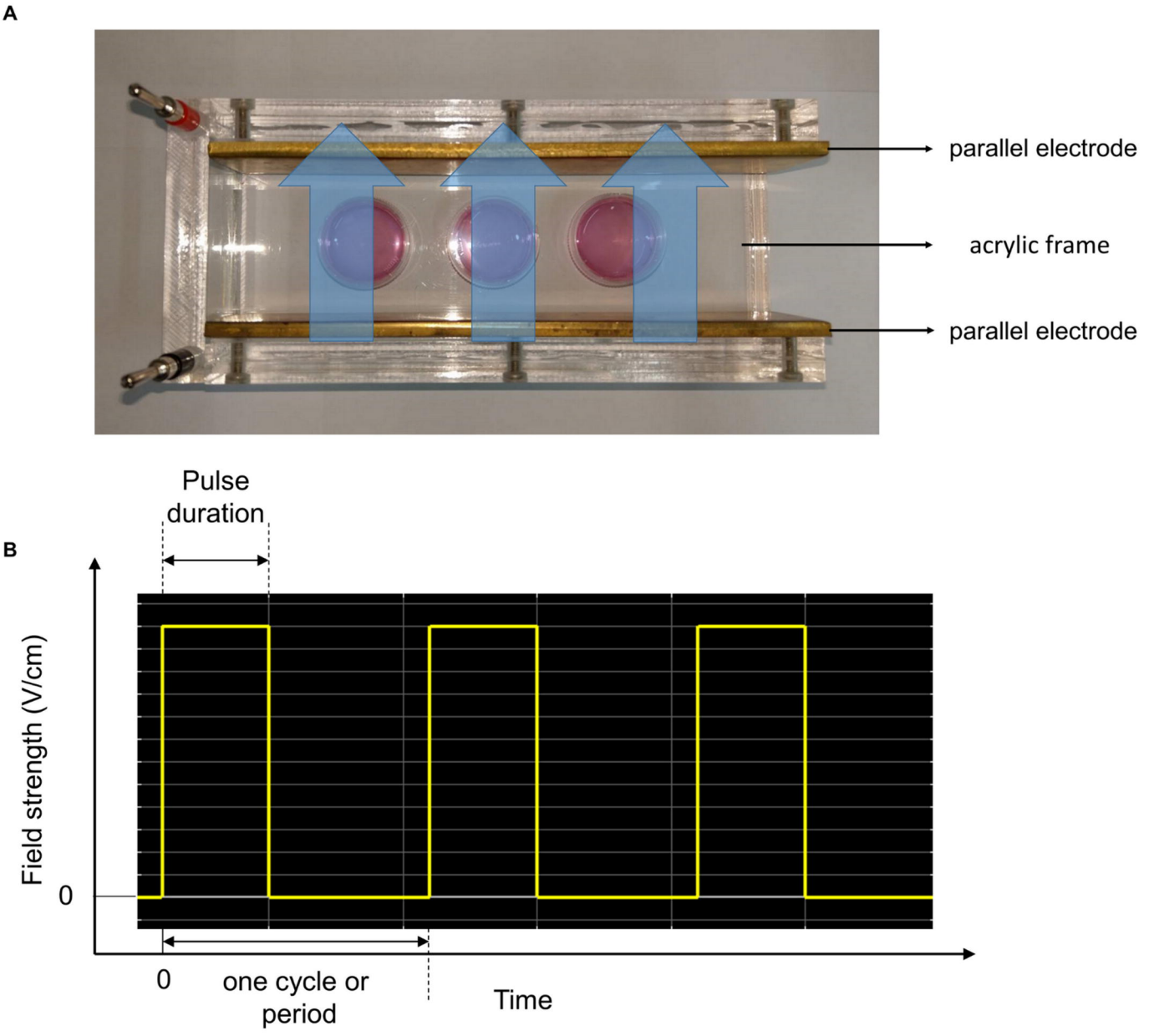
A
parallel electrode
acrylic frame
parallel electrode
B
Pulse duration
Field strength (V/cm)
0
0
one cycle or period
Time

Figure 2

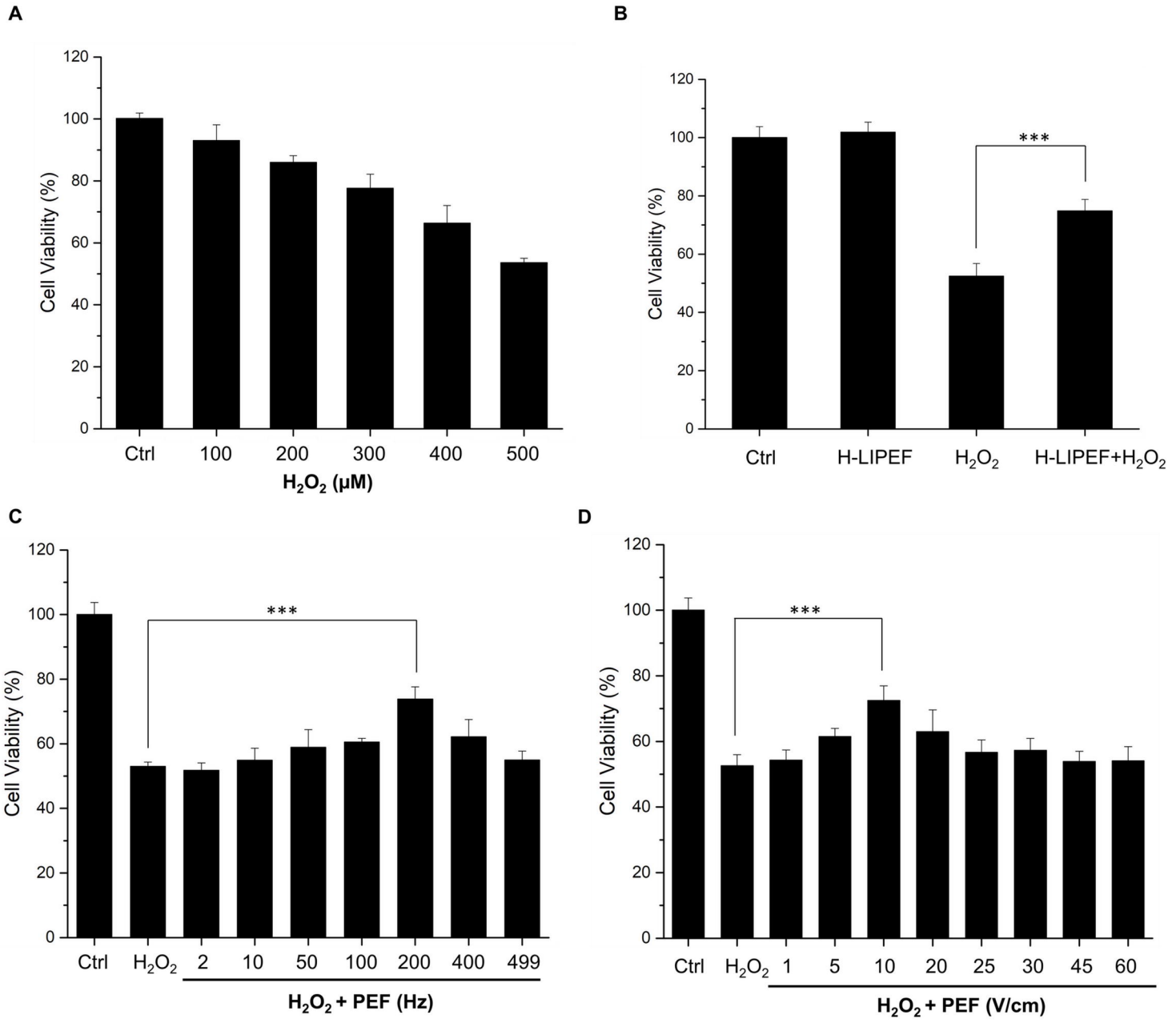
A
Cell Viability (%)
120
100
80
60
40
20
0
Ctrl
100
200
300
400
500
H2O2 (μM)
B
Cell Viability (%)
***
Ctrl
H-LIPEF
H2O2
H-LIPEF+H2O2
C
Cell Viability (%)
***
Ctrl
H2O2
2
10
50
100
200
400
499
H2O2 + PEF (Hz)
D
Cell Viability (%)
***
Ctrl
H2O2
1
5
10
20
25
30
45
60
H2O2 + PEF (V/cm)

Figure 3

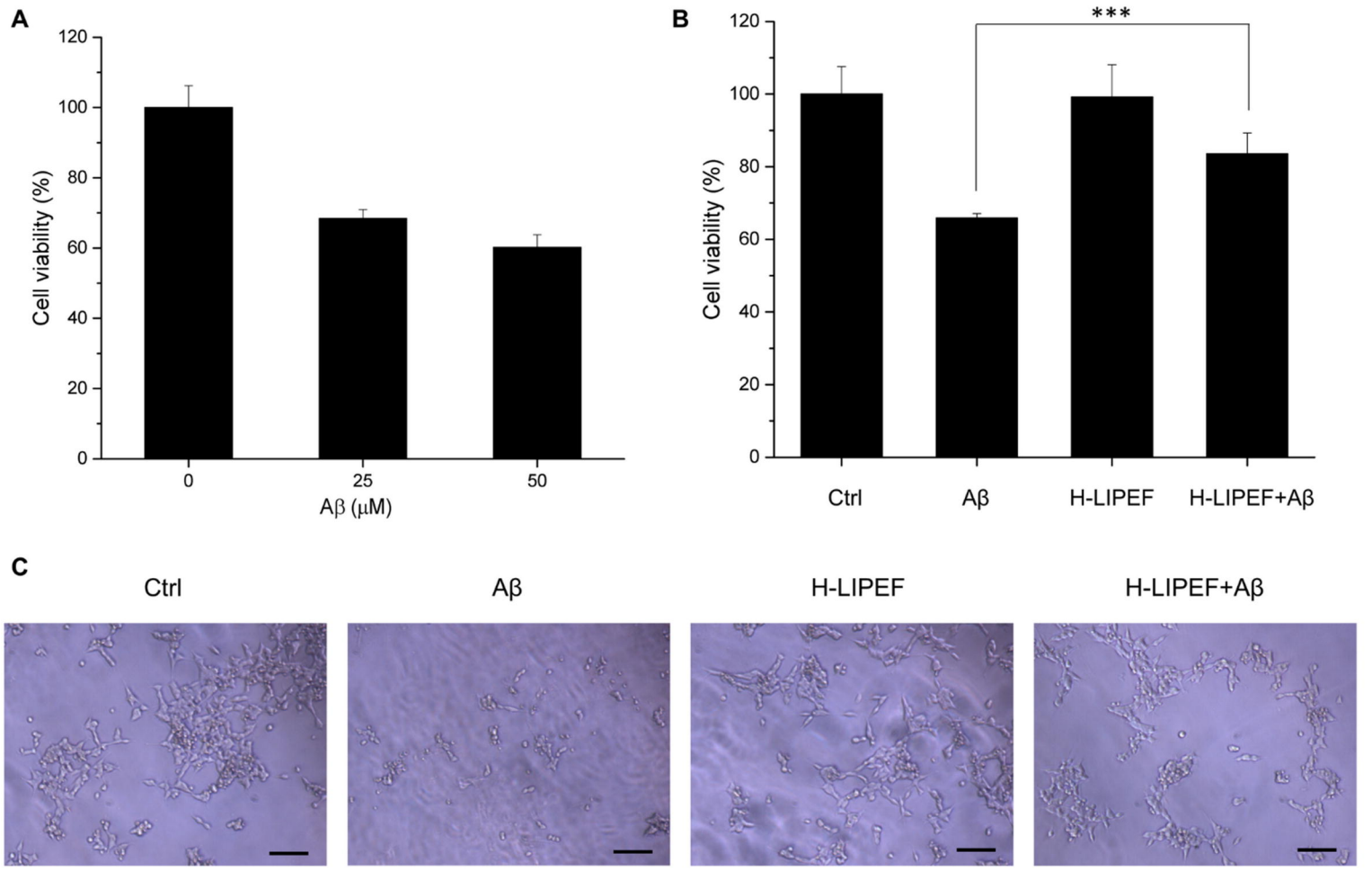
A
Cell viability (%)
120
100
80
60
40
20
0
0
25
50
Aβ (μM)
B
***
Cell viability (%)
120
100
80
60
40
20
0
Ctrl
Aβ
H-LIPEF
H-LIPEF+Aβ
C
Ctrl
Aβ
H-LIPEF
H-LIPEF+Aβ

Figure 4

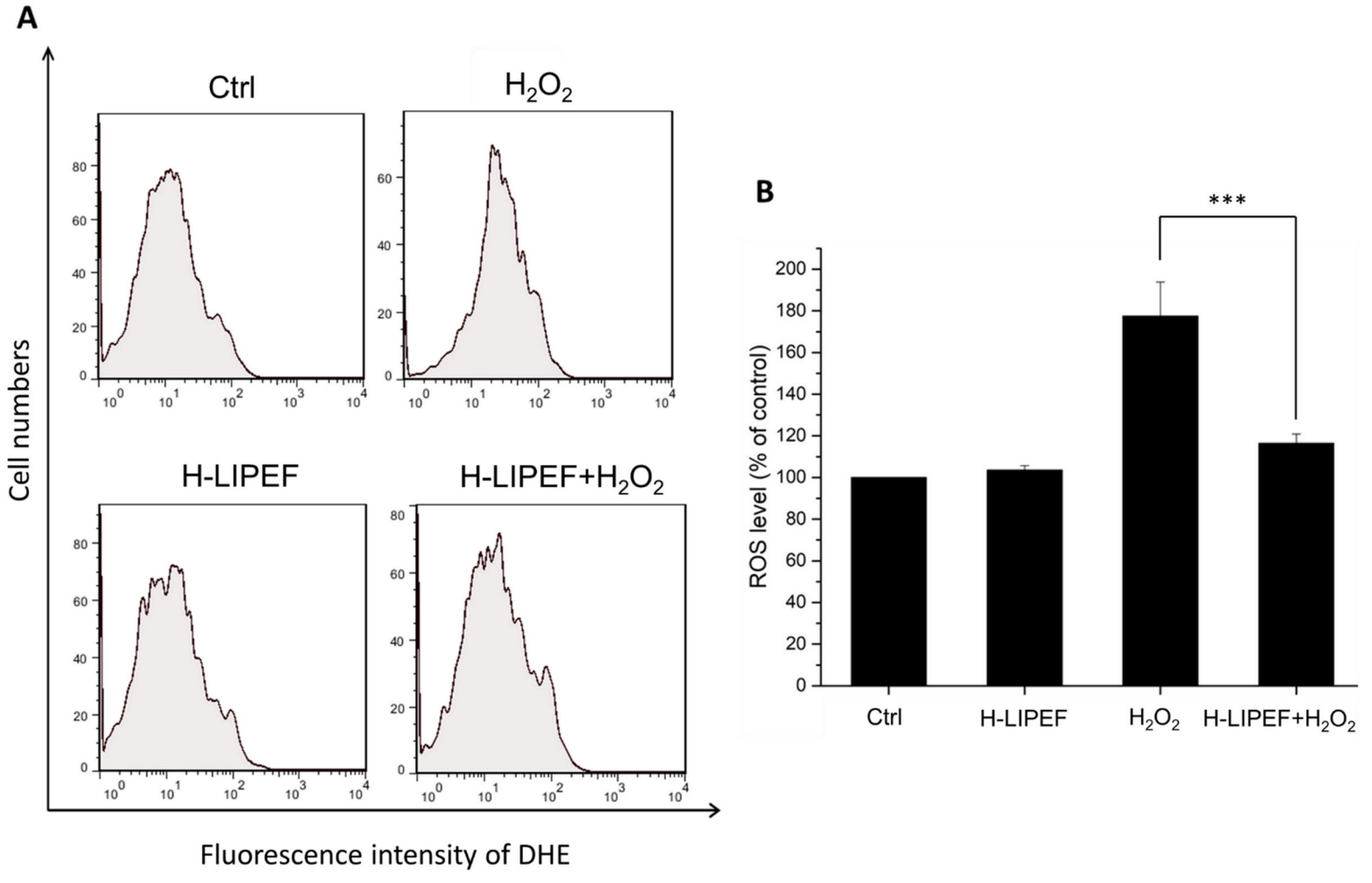
A
Ctrl
H_2O_2
H-LIPEF
H-LIPEF+H_2O_2
Cell numbers
Fluorescence intensity of DHE
B
***
ROS level (% of control)
Ctrl
H-LIPEF
H_2O_2
H-LIPEF+H_2O_2

Figure 5

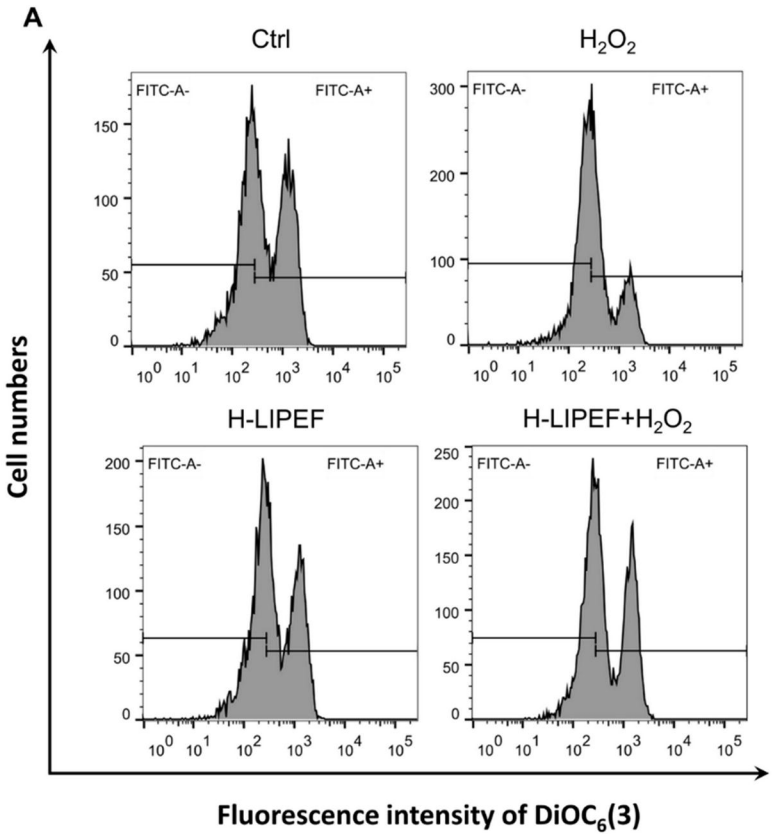
A
Ctrl
H_2O_2
H-LIPEF
H-LIPEF+H_2O_2
FITC-A-
FITC-A+
Cell numbers
Fluorescence intensity of $DiOC_6(3)$

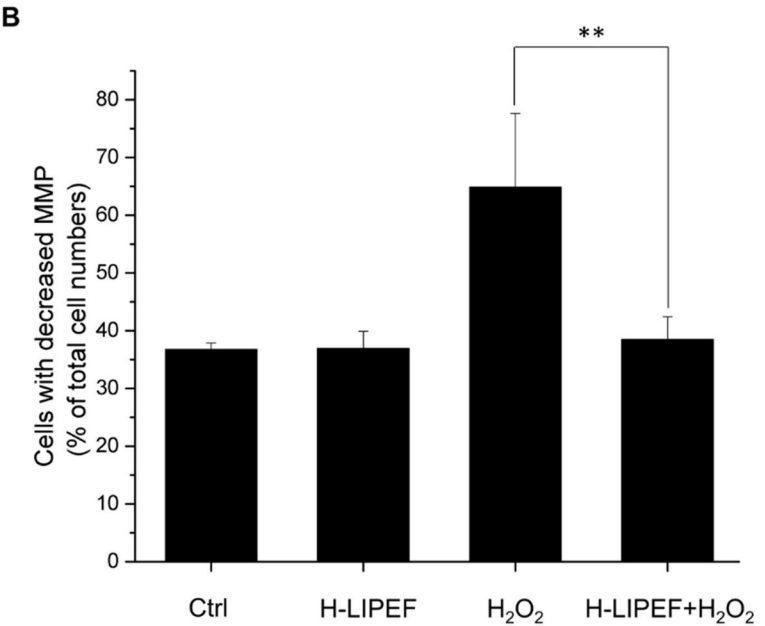
B
**
Cells with decreased MMP
(% of total cell numbers)
Ctrl
H-LIPEF
H_2O_2
H-LIPEF+H_2O_2

Figure 6

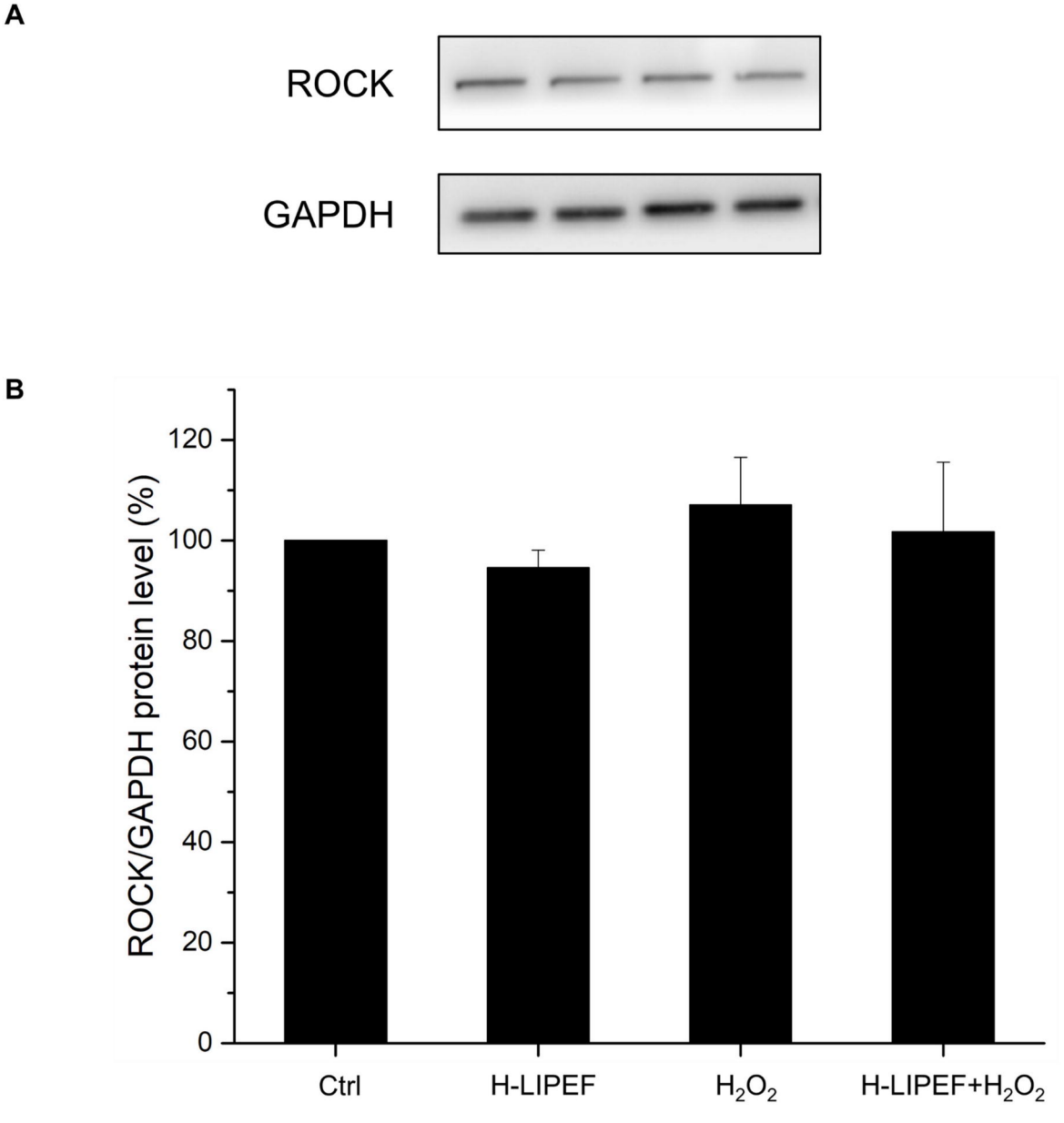
A
ROCK
GAPDH
B
ROCK/GAPDH protein level (%)
0
20
40
60
80
100
120
Ctrl
H-LIPEF
H_2O_2
H-LIPEF+H_2O_2

Figure 7

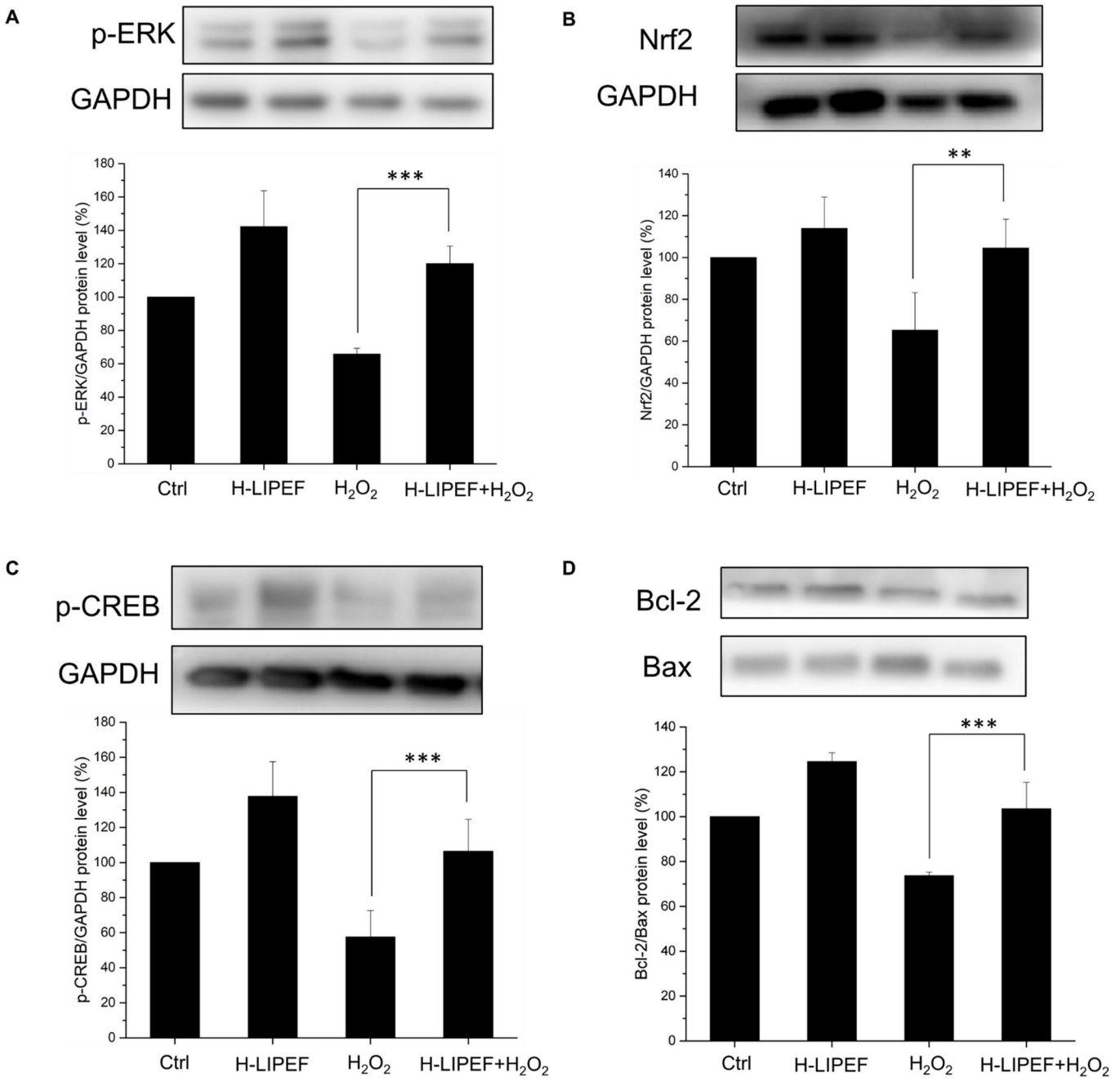
A
p-ERK
GAPDH
p-ERK/GAPDH protein level (%)
***
Ctrl
H-LIPEF
H2O2
H-LIPEF+H2O2
B
Nrf2
GAPDH
Nrf2/GAPDH protein level (%)
**
Ctrl
H-LIPEF
H2O2
H-LIPEF+H2O2
C
p-CREB
GAPDH
p-CREB/GAPDH protein level (%)
***
Ctrl
H-LIPEF
H2O2
H-LIPEF+H2O2
D
Bcl-2
Bax
Bcl-2/Bax protein level (%)
***
Ctrl
H-LIPEF
H2O2
H-LIPEF+H2O2

Figure 8

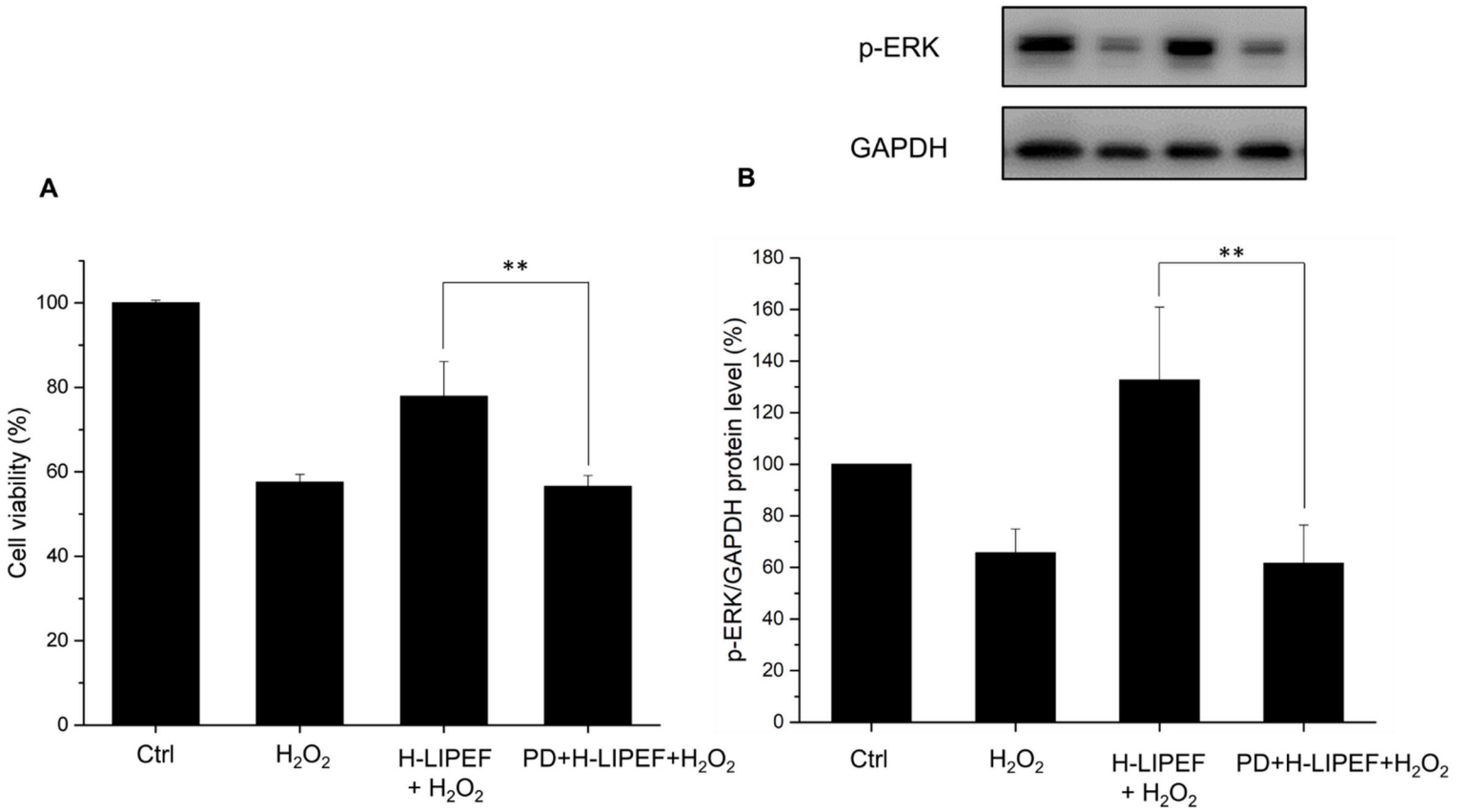
A
Cell viability (%)
0
20
40
60
80
100
**
Ctrl
H_2O_2
H-LIPEF + H_2O_2
PD+H-LIPEF+H_2O_2
B
p-ERK
GAPDH
p-ERK/GAPDH protein level (%)
0
20
40
60
80
100
120
140
160
180
**
Ctrl
H_2O_2
H-LIPEF + H_2O_2
PD+H-LIPEF+H_2O_2